THE OFFICIAL MAGAZINE OF THE OCEANOGRAPHY SOCIETY

Oceanography

CITATION

Jones, B.H., and Y. Kattan. 2017. KAUST's Red Sea observing system. *Oceanography* 30(2):53–55, https://doi.org/10.5670/oceanog.2017.221.

DOI

https://doi.org/10.5670/oceanog.2017.221

KAUST's Red Sea Observing System

By Burton H. Jones and Yasser Kattan

A combination of thermohaline circulation and monsoon-modulated winds drive advection in the Red Sea. Biogeochemical processes are closely coupled with the physical dynamics of the sea, yet to date remain poorly resolved and understood. Given the Red Sea's size (~2,000 km × 250 km), frequently occurring eddies can provide a mechanism for significant exchange between the open sea and its abundant coastal coral reef regions. Because no international waters exist within the Red Sea, and geopolitical restrictions allow only limited access, our most complete understanding of the Red Sea until recently has come from remote sensing and numerical modeling studies (e.g., Sofianos and Johns, 2002; Raitsos et al., 2013; Yao et al, 2014; Racault et al., 2015), although occasional ship expeditions have provided in situ observations with limited temporal and/or spatial coverage (e.g., Naqvi et al., 1986; Sofianos and Johns, 2007; Bower and Farrar, 2015; Kürten et al., 2016).

To better understand the physical and biogeochemical characteristics of the Red Sea, King Abdullah University of Science and Technology's (KAUST's) Integrated Ocean Processes (IOP) laboratory is employing autonomous platforms coupled with coastal surface current mapping systems. The sustained, quasi-synoptic view provided by the data collected will permit IOP to address the following questions:

- What is the annual cycle of physical and biogeochemical variability in the Red Sea?
- What are the roles of mesoscale and submesoscale eddies in structuring the physical and biogeochemical dynamics of the Red Sea?
- How do winter mixing, convection, and related eddy activity affect Red Sea circulation and biogeochemical processes?
- What are the distribution and variability of the transport and what are the forcing functions that determine the Red Sea basin's transport?

The observing elements consist of (1) autonomous underwater gliders distributed along three sampling lines (Figure 1), (2) three profiling Biogeochemical-Argo floats, and (3) coastal surface current mapping using high-frequency radar operating at 16 MHz (CODAR; Figure 1). The floats, although not indicated on the Figure 1 map, were deployed in the central (one float) and northern (two floats) Red Sea. The three glider lines are intended to provide sustained observations that will yield insights into the seasonal, annual, and interannual scales of variability in the Red Sea, and enable evaluation of the role of along-basin transport. Instrumentation on the autonomous platforms provides measurements of temperature, salinity, dissolved oxygen, chlorophyll, chromophoric dissolved organic matter (CDOM) fluorescence, and multi-wavelength optical backscatter; two of the floats also measure downwelling irradiance at four wavelengths. CODAR pairs, each of which covers an area approximately 100 km in diameter, are located in the north near Duba, in the central Red Sea between KAUST and Rabigh, and in the southern Red Sea, north of Jazan.

Several criteria were used in selecting the locations for observations. First, each must be a region where significant oceanographic processes occur that are essential for understanding the overall dynamics of the Red Sea. Second, the region must have socioeconomic importance because of existing urban and industrial activities or significant planned or already underway development, such as near Jazan in the south. Third, the region must meet the very practical need for access to maintenance facilities and areas where ship-based observations can be made.

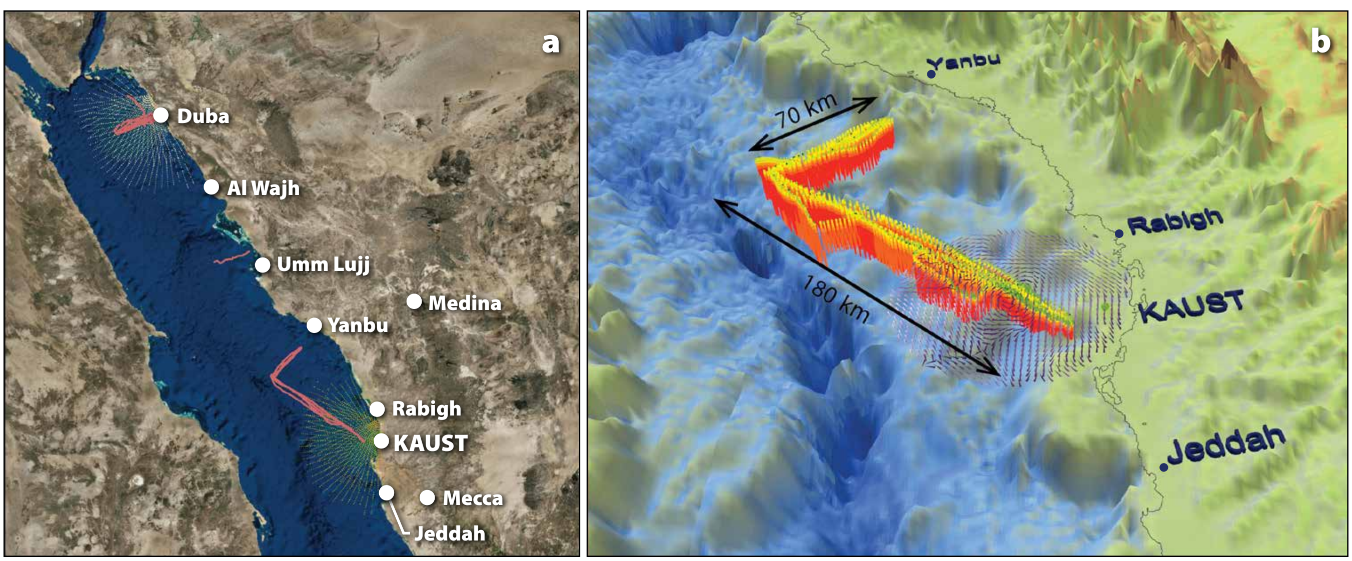

FIGURE 1. (a) Areas of surface current mapping and glider deployments in the Red Sea. Another surface current mapping region lies to the south, near the new development of Jazan Economic City. (b) Southern region of (a) in more detail, showing the overlap between surface current mapping and the central Red Sea sustained glider line projected on a topographic map of the region. The colors on the glider profiles represent salinity, ranging from 39 (blue) to 40.6 (red). The maximum profile depth is 900 m. The surface current mapping areas in panel a, located near Duba in the north and in the central Red Sea between KAUST and Rabigh, cover areas that extend about 100 km offshore and 100 km alongshore.

Ship-based efforts supplement the autonomous platform observations. These in situ biological, chemical, and optical measurements both validate the autonomously gathered data and provide measurements that cannot be obtained by the autonomous platforms. The ship-based measurements have already yielded insights into major gradients in plankton species composition and its variability in the Red Sea, into trophic interactions, and into the role of physical processes in transporting waters into the Red Sea, especially from the Gulf of Aden. Stratification and eddies that occur along much of the sea are also subjects of ship-based investigations (Kürten et al., 2016; Kheireddine et al., 2017; Pearman et al., 2017).

To illustrate this point, glider observations and surface current mapping in the north central Red Sea have validated the presence and influence of the eastern boundary current (EBC). Models show the EBC to be a relatively persistent feature in the region (e.g., Sofianos and Johns, 2003; Yao et al., 2014), but validation of the EBC and its role in the transport of Gulf of Aden surface and/or intermediate water (GASW and GAIW, respectively) has until recently been limited (e.g., Churchill et al., 2014). Figure 1 shows the glider coverage areas. Velocity vectors from surface current mapping (Figure 2a) and from sustained glider observations (Figure 2b) show the presence of a nearshore current both within the CODAR coverage area and about 160 km to the north where the glider provides coverage. One of the contributions of the northward EBC is the transport of inflow water from the Gulf of Aden, the Red Sea's primary connection with the global ocean. In the glider section, two components of Gulf of Aden inflow are evident. Near the coast in the region of northward flow, a warm, low-salinity water mass is evident in the surface layer (Figure 3, indicated by the black ellipse). This water mass is identified as GASW that typically enters the Red Sea from September through May (Sofianos and Johns, 2015). Farther offshore, westward of 37.7°E, a thin lower salinity and higher chlorophyll layer is observed between 50 m and 80 m depth. This layer is consistent with GAIW that enters the Red Sea from June to September. Churchill et al. (2014) show that in the southern Red Sea, this low-salinity water is elevated in chlorophyll, low in oxygen, and enriched in inorganic nutrients. By the time this water reaches this latitude in the Red Sea, its signature has weakened due to mixing and biological productivity that occur during its northward transit. However, this advection of the GAIW into the northern half of the Red Sea contributes to the region's productivity, which is otherwise limited by high stratification from spring through fall. A submesoscale cyclonic eddy can be seen immediately west of the GASW. Such eddies appear to be relatively common occurrences along the eastern boundary of the Red Sea. Zarokanellos et al. (2017) discussed the presence of mesoscale eddies and their interaction with the EBC during the winter-summer transition using a combination of ship observations and our earliest glider observations. These eddies are important in steering or blocking the northward transport of the EBC along its northward transit.

The observations obtained to date are already yielding significant insights into the functioning of the Red Sea. The effort will be sustained and, if resources permit, expanded to continue the development of a holistic view of Red Sea dynamics, including responses to interannual and longer-term processes as well as global change phenomena.

REFERENCES

Bower, A.S., and J.T. Farrar. 2015. Air–sea interaction and horizontal circulation in the Red Sea. Pp. 329–342 in *The Red Sea: The Formation, Morphology, Oceanography and Environment of a Young Ocean Basin*. N.M.A. Rasul and I.C.F. Stewart, eds, Springer Berlin Heidelberg, https://doi.org/10.1007/978-3-662-45201-1_19.

Churchill, J.H., A.S. Bower, D.C. McCorkle, and Y. Abualnaja. 2014. The transport of nutrient-rich Indian Ocean water through the Red Sea and into coastal reef systems. *Journal of Marine Research* 72(3):165–181.

Kheireddine, M., M. Ouhssain, H. Claustre, J. Uitz, B. Gentili, and B.H. Jones. 2017. Assessing pigment-based phytoplankton community distributions in the Red Sea. *Frontiers in Marine Science* 4:132, https://doi.org/10.3389/fmars.2017.00132.

Kürten, B., A.M. Al-Aidaroos, S. Kürten, M.M. El-Sherbiny, R.P. Devassy, U. Struck, N. Zarokanellos, B.H. Jones, T. Hansen, G. Bruss, and U. Sommer. 2016. Carbon and nitrogen stable isotope ratios of pelagic zooplankton elucidate ecohydrographic features in the oligotrophic Red Sea. *Progress in Oceanography* 140:69–90, https://doi.org/10.1016/j.pocean.2015.11.003.

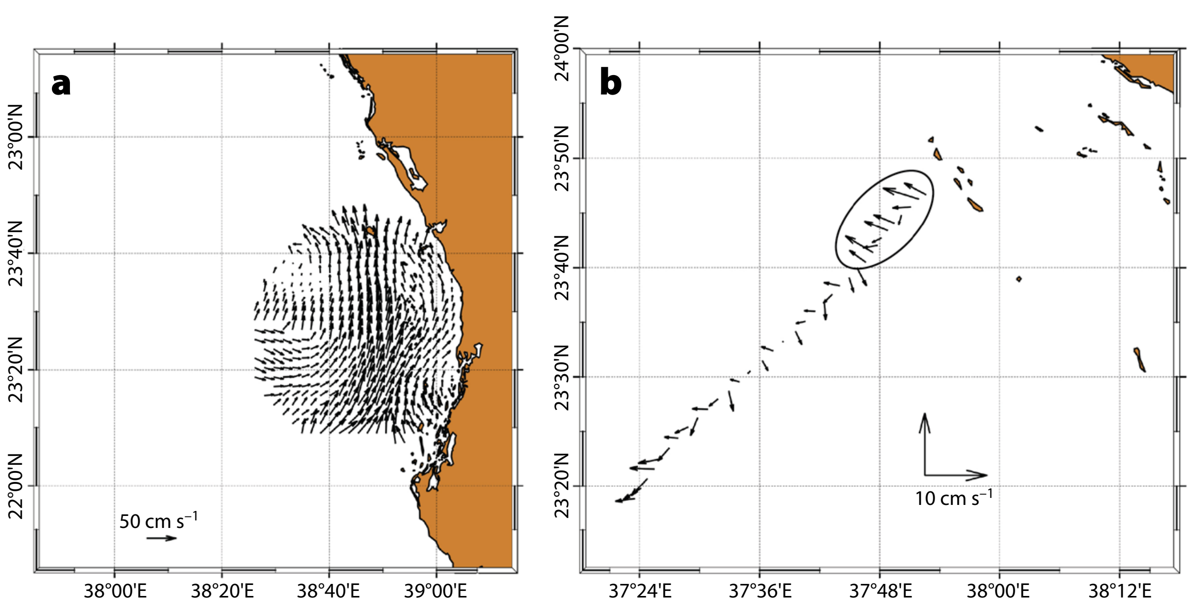

FIGURE 2. Coastal velocities mapped by (a) high-frequency radar (CODAR) for the period of June 14–16, 2017, and (b) glider displacement measurements from a section run October 23–29, 2015. The high-frequency radar measurements are surface currents, and the glider measurements are water column velocities integrated between the surface and about 600–700 m depth.

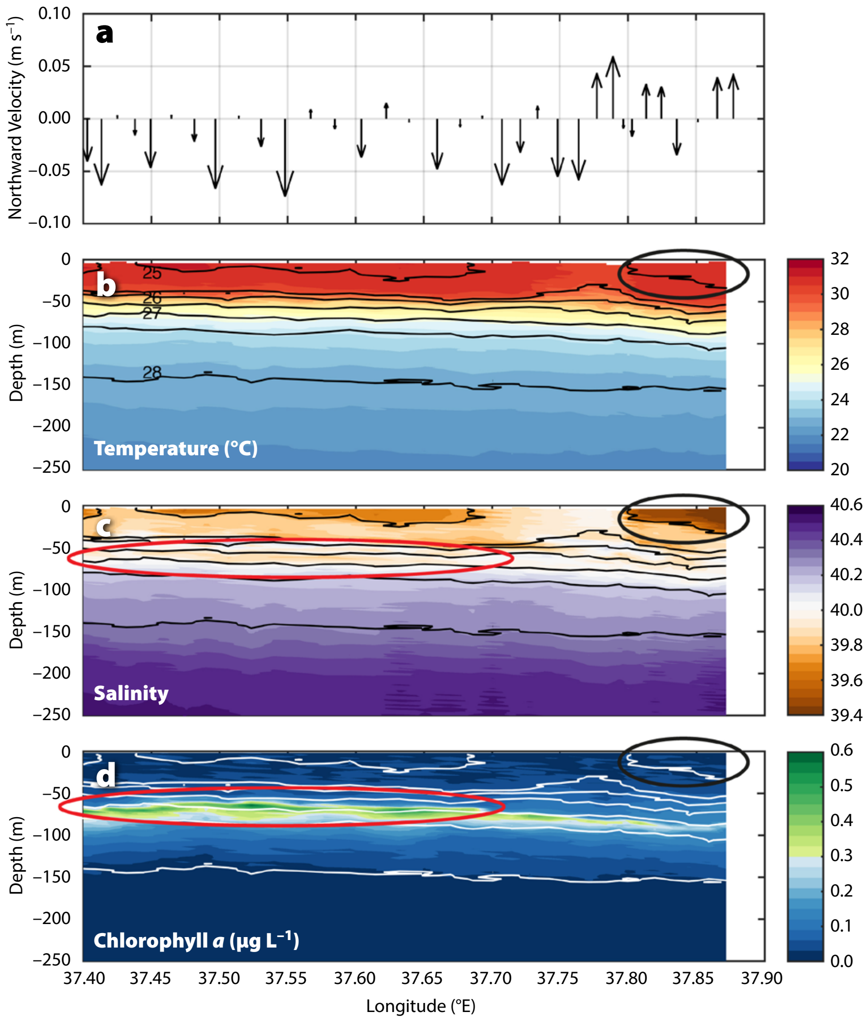

FIGURE 3. Glider section perpendicular to the coast southwest from Yanbu (see Figure 1). (a) The northward component of the integrated water column velocity. (b) Temperature distribution. (c) Salinity. (d) Chlorophyll concentration. The black ellipse in the upper right corner of the temperature, salinity, and chlorophyll panels outlines Gulf of Aden Surface Water (GASW) advecting northward. The red ellipses outline low-salinity, high-chlorophyll water that is consistent with Gulf of Aden Intermediate Water (GAIW) advecting northward. The density anomaly (kg m^{-3}) is represented in the bottom three panels by contour lines whose values are shown in the temperature panel.

Naqvi, S.W.A., H.P. Hansen, and T.W. Kureishy. 1986. Nutrient uptake and regeneration ratios in the Red Sea with reference to the nutrient budgets. *Oceanologica Acta* 9(3):271–275.

Pearman, J.K., J. Ellis, X. Irigoien, Y.V.B. Sarma, B.H. Jones, and S. Carvalho. 2017. Microbial planktonic communities in the Red Sea: High levels of spatial and temporal variability shaped by nutrient availability and turbulence. *Scientific Reports* 7, 6611, https://doi.org/10.1038/s41598-017-06928-z.

Racault, M.-F., D.E. Raitsos, M.L. Berumen, R.J.W. Brewin, T. Platt, S. Sathyendranath, and I. Hoteit. 2015. Phytoplankton phenology indices in coral reef ecosystems: Application to ocean-color observations in the Red Sea. *Remote Sensing of Environment* 160:222–234, https://doi.org/10.1016/j.rse.2015.01.019.

Raitsos, D.E., Y. Pradhan, R.J.W. Brewin, G. Stenchikov, and I. Hoteit. 2013. Remote sensing the phytoplankton seasonal succession of the Red Sea. *PLOS One* 8(6), e64909, https://doi.org/10.1371/journal.pone.0064909.

Sofianos, S.S., and W.E. Johns. 2002. An Oceanic General Circulation Model (OGCM) investigation of the Red Sea circulation: Part 1. Exchange between the Red Sea and the Indian Ocean. *Journal of Geophysical Research* 107(C11), 3196, https://doi.org/10.1029/2001jc001184.

Sofianos, S.S., and W.E. Johns. 2003. An Oceanic General Circulation Model (OGCM) investigation of the Red Sea circulation: Part 2. Three-dimensional circulation in the Red Sea. *Journal of Geophysical Research* 108, 3066, https://doi.org/10.1029/2001JC001185.

Sofianos, S.S., and W.E. Johns. 2007. Observations of the summer Red Sea circulation. *Journal of Geophysical Research* 112, C06025, https://doi.org/10.1029/2006jc003886.

Sofianos, S., and W.E. Johns. 2015. Water mass formation, overturning circulation, and the exchange of the Red Sea with the adjacent basins. Pp. 343–353 in *The Red Sea: The Formation, Morphology, Oceanography and Environment of a Young Ocean Basin*. N.M.A. Rasul and I.C.F. Stewart, eds, Springer Berlin Heidelberg, https://doi.org/10.1007/978-3-662-45201-1_20.

Yao, F.C., I. Hoteit, L.J. Pratt, A.S. Bower, P. Zhai, A. Kohl, and G. Gopalakrishnan. 2014. Seasonal overturning circulation in the Red Sea: Part 1. Model validation and summer circulation. *Journal of Geophysical Research* 119(4):2,238–2,262, https://doi.org/10.1002/2013jc009004.

Zarokanellos, N.D., V.P. Papadopoulos, S.S. Sofianos, and B.H. Jones. 2017. Physical and biological characteristics of the winter-summer transition in the Central Red Sea. *Journal of Geophysical Research*, https://doi.org/10.1002/2017JC012882.

ACKNOWLEDGMENTS

This research is funded by King Abdullah University of Science and Technology and Saudi Aramco's Environmental Protection Division. Ute Langner provided the GIS projections, Lohitzune Solabarietta provided the CODAR image, and Nikolaos Zarokanellos provided the glider data and assisted with its preparation. Jennifer Otoadese assisted with editing of the manuscript.

AUTHORS

Burton H. Jones (burton.jones@kaust.edu.sa) is Professor, King Abdullah University of Science and Technology, Thuwal, Saudi Arabia. **Yasser Kattan** is Senior Environmental Consultant, Environmental Protection Department, Saudi Aramco, Dahran, Saudi Arabia.

ARTICLE CITATION

Jones, B.H., and Y. Kattan. 2017. KAUST's Red Sea observing system. *Oceanography* 30(2):53–55, https://doi.org/10.5670/oceanog.2017.221.